SPE 119166

Phase Equilibrium Computations Are No Longer the Bottleneck in Thermal Compositional EoS Based Simulation

A. Iranshahr, D.V. Voskov and H.A. Tchelepi, Stanford University

Abstract

Thermodynamic equilibrium computations are usually the most time consuming component in compositional reservoir flow simulation. A Compositional Space Adaptive Tabulation (CSAT) approach has been developed as a preconditioner for Equation of State (EoS) computations in isothermal compositional simulation. The compositional space is decomposed into sub- and super-critical regions. In the sub-critical region, we adaptively parameterize the compositional space using a small number of tie-lines, which are assembled into a table. The critical surface is parameterized and used to identify super-critical compositions. The phase equilibrium information for a composition is interpolated as a function of pressure using the tie-line table. We extend the CSAT approach to thermal problems. Given an overall composition at a fixed temperature, the boundary between sub- and super-critical pressures is represented by the critical tie-line and the corresponding minimal critical pressure. A small set of sub-critical tie-lines is computed and stored for a given temperature. This process is repeated for the pressure and temperature ranges of interest, and a coarse (regular) tie-line table is constructed. Close to the critical boundary, a refined tie-line table is used. A combination of regular and refined interpolation improves the robustness of the tie-line search procedure and the overall efficiency of the computations. Several challenging problems, including an unstructured heterogeneous discrete fracture field model with 26 components, are used to demonstrate the robustness and efficiency of this general tie-line based parameterization method. Our results indicate that CSAT provides very accurate treatment of the near-critical region. Moreover, the computational efficiency of the method is at least an order of magnitude better than that of standard EoS-based reservoir simulation approaches. We also show the efficiency gains relative to standard techniques as a function of the number of gridblocks in the simulation model.

Introduction

Thermal recovery and gas injection processes are among the most commonly used Enhanced Oil Recovery (EOR) methods. Due to the complexity of their models, accurate and efficient simulation of thermal-compositional processes is the target of active research.

Farouq Ali and Abou-Kassem (1988) presented a detailed description of the complex physical mechanisms and various numerical models for thermal recovery processes. A comprehensive review of the numerical considerations in general-purpose reservoir simulation models was presented by Wong and Aziz (1988). For a general thermal-compositional simulation model, the energy balance equation as well as species conservation equations must be discretized and solved. Simultaneous solution of the energy and mass conservation equations was first demonstrated by Coats et al. (1974). Their numerical model solved the three-phase flow of oil, water, and steam for a steam-flooding problem. Their model assumed that only the water and steam phases exchange mass. Later, Coats (1976) extended this formulation by modeling steam distillation of oil and release of solution gas. In his model, a fixed number of conservation equations is solved, where oil is represented as a mixture of solution gas, a distillable portion and nonvolatile heavy ends. Moreover, Coats assumed that the phase equilibrium ratios are functions of pressure and temperature only. Natural variables (pressure, temperature, phase saturations, and component mole fractions) were used in the formulation.

Chien et al. (1989) developed a three-phase thermal compositional simulator with the objective of higher computational speed. They used vectorization to improve computational efficiency and represented the thermodynamic phase behavior by an Equation of State (EoS) to achieve a thermodynamically consistent model. Their model used pressure, temperature and overall component mole fractions as primary variables. Brantferger et al. (1991) proposed enthalpy, in place of temperature, as a primary variable. Their formulation eliminates the need to use variable substitution when temperature and pressure become dependent as a result of component disappearance due to distillation. Because of the choice of the primary variables, Brantferger et al. implemented an isenthalpic flash procedure to model instantaneous phase equilibrium within each gridblock.

The EoS calculations performed along with the solution of conservation equations (using natural variables) include stability testing and flash procedures for single- and multi-phase states, respectively. In most simulators, the phase stability step can become the dominant kernel in EoS computations. To speedup standard EoS calculations, a Method of Characteristics (MoC) based approach for two-phase multi-component displacements has been derived for ideal problems, where tie-lines are used to construct the solution path in compositional space. Orr (2007) provides a detailed description of the development of this approach. Although the MoC theory is applicable to ideal settings (namely, constant pressure displacement in a one-dimensional homogeneous porous medium without dispersion), it clearly indicates that the properties of compositional gas injection processes are determined by a set of key tie-lines between the injection and initial compositions. The key tie-lines are connected to each other by shocks and rarefactions. Helfferich (1981) developed a generalized mathematical theory for multicomponent, multiphase displacements in porous media. Monroe et al. (1990) reported the first solution for a four-component system. A number of authors have studied the effects of volume change as a result of component transfer between phases (see Dindoruk et al. (1992)). Wang and Orr (1997) generalized the solution to systems with an arbitrary number of components, assuming that adjacent key tie-lines are connected by shocks only. Jessen et al. (1999) introduced the idea of primary key tie-lines and developed a methodology to determine the existence of rarefactions in the solution. Voskov and Entov (2001) presented a nonlinear decoupling of the thermodynamic and hydrodynamic problems, and Zhu (2003) developed analytical solutions for problems with temperature variation.

Although MoC theory is based on one-dimensional dispersion-free flow, it has improved our knowledge of the thermodynamic and hydrodynamic interactions in compositional porous media flows. Motivated by this theory, a tie-line based parameterization method has been developed, which treats the thermodynamic portion of the problem using tie-lines rather than the conventional representation of the compositional space (Entov, 1997; Entov et al., 2001; Voskov and Entov, 2001; Voskov, 2002). An isothermal Compositional Space Adaptive Tabulation (CSAT) methodology for two-phase displacements was presented recently (Voskov and Tchelepi, 2007, 2008a,b), which has been extended to equilibrium computations with an arbitrary number of phases (Voskov and Tchelepi, 2008c). The CSAT framework has proven to be effective for realistic compositional problems. In this work, we extend the CSAT methodology to thermal problems with emphasis on the efficiency of the phase-behavior representation.

After a brief overview of the concepts of the isothermal compositional space parameterization methodology, we describe the extension of the CSAT approach to thermal problems. Application of isothermal CSAT to large-scale problems is then presented, which is followed by a variety of simulation cases for thermal-compositional problems. We then present preliminary results for compositional space parameterization of three-phase thermal compositional simulation.

Compositional Space Adaptive Tabulation

The component and energy conservation equations for a gridblock containing N_c components and N_{ph} phases are written as:

$$\frac{\partial}{\partial t}\left(\phi \sum_j x_{i,j}\rho_j S_j\right) - \nabla.\left(\sum_j x_{i,j}\rho_j \mathbf{u}_j\right) + \sum_j x_{i,j}\rho_j q_j = 0, \qquad i \in \{1, N_c\}, \tag{1}$$

$$\frac{\partial}{\partial t}\left(\phi \sum_j U_j\rho_j S_j + (1-\phi)U_R\right) - \nabla.\left(\sum_j H_j\rho_j \mathbf{u}_j + \kappa\nabla T\right) + \sum_j H_j\rho_j q_j = 0, \qquad i \in \{1, N_c\}. \tag{2}$$

In standard natural-variable compositional simulators, a dynamic formulation of the conservation equations accounts for the appearance and disappearance of phases in the displacement. For gridblocks in a multiphase state, equality equations for component fugacities are solved with the conservation equations in a global Newton iteration. If the saturation of a phase in a gridblock becomes negative, the conservation equations are solved with that phase removed. On the other hand, for gridblocks in a single-phase state, phase stability testing is performed to determine if the fluid is thermodynamically stable under the new prevailing conditions. If the mixture is found to be unstable, a flash procedure computes the equilibrium phase ratios and the properties of the phases. Obviously, a consistent multi-phase formulation of the conservation laws is required for such gridblocks. A detailed discussion of standard EoS computations can be found in Michelsen (1982a,b).

The idea of compositional space parameterization for multiphase multicomponent flow and transport in porous media is based on the fact that the majority of standard EoS computations that are performed to determine the thermodynamic

state of the gridblocks are redundant. From MoC theory, we know that compositions in the single phase region that are connected to points in the two-phase region, lie along key tie-lines that are extended through the injection and initial compositions (Orr, 2007). Hence, tie-lines can be used to parameterize the composition path of the displacement. (This parameterization is around compositions in the single-phase state) For real problem settings, where compositions along the numerical solution path are smeared due to dispersion effects (both physical and numerical), tie-lines also prove to be an efficient parameterization strategy (Voskov and Tchelepi, 2008a).

Parameterization of the entire compositional space for the pressure range of interest is both expensive and unnecessary. The CSAT (Compositional Space Adaptive Tabulation) method adaptively picks the composition points in the course of the simulation and parameterizes the space around them (Voskov and Tchelepi, 2007, 2008a,b). A composition (called *base point*) is selected for *tie-line tabulation*, if it is not close to existing tie-lines. Moreover, since adjacent composition points have different pressures, tie-lines through the base point are computed and stored at discrete pressure values. Consequently, *interpolation* in pressure is required to obtain an estimate of the tie-line that parameterizes other compositions (called *test points*). The following criterion is used to verify the closeness of the interpolated tie-line to a test point (with compositions represented by $(\bar{x}, \bar{y})$ and z, respectively):

$$\sqrt{\sum_{i=1}^{N_c}(z_i - \bar{x}_i L - \bar{y}_i(1-L))^2} < \varepsilon, \tag{3}$$

for some user-defined ε and with $L = (z_k - \bar{y}_k)/(\bar{x}_k - \bar{y}_k)$, where k is the index of the component with maximum overall composition.

The minimal pressure for which the composition is intersected by a critical tie-line, is called the Minimal Critical Pressure (MCP). A tie-line is defined as trivial, if it satisfies:

$$\varepsilon_{min} < \ell_{tie\text{-}line} \equiv \sqrt{\sum_{i=1}^{N_c}(x_i - y_i)^2} < \varepsilon_{max}, \tag{4}$$

for some ε_{min} and ε_{max}, where ℓ is the length of the tie-line in compositional space. A refined pressure grid is constructed below the MCP to improve the interpolation for multi-contact miscible displacements. In order to parameterize compositions in the super-critical space, a Super-critical State Criteria (SSC) is developed, which parameterizes the space in terms of critical tie-lines. For the full details of this isothermal methodology, refer to Voskov and Tchelepi (2007, 2008a,b).

Tie-Line Parameterization for Thermal Problems

When energy conservation is also considered along with the system of flow and transport equations, treatment of the thermodynamic phase behavior becomes more complicated due to changes in both pressure and temperature . Considering the fact that p and T are independent variables, we use them as our primary variables for tie-line tabulation and interpolation. We first extend the isothermal parameterization methodology to thermal immiscible displacements. Then, after considering first-contact miscible problems, we combine the two schemes to obtain a general-purpose methodology.

The parameterization techniques of isothermal compositional simulation (Voskov and Tchelepi, 2007, 2008a,b) can be extended for thermal problems as follows. Lower and upper bounds for p and T (denoted by p_{min}, p_{max}, T_{min} and T_{max}), as well as the number of discretization points in both variables (denoted by N_p and N_T) are determined by the user. This information defines the coarse $p - T$ grid over which tie-lines through a given composition (base point) are computed:

$$(p_{i_p}, T_{i_T}) = (p_{min} + i_p \Delta p, T_{min} + i_T \Delta T), \qquad 0 \le i_{p,T} \le N_{p,T} - 1, \tag{5}$$

where,

$$\Delta p = \frac{p_{max} - p_{min}}{N_p - 1}, \tag{6}$$

$$\Delta T = \frac{T_{max} - T_{min}}{N_T - 1}. \tag{7}$$

For each temperature value and starting from p_{min}, tie-lines through the base point are calculated at discrete pressure values until either the MCP for the current T, or the maximum allowable pressure, p_{max}, is reached. Following the same procedure for all discrete temperature values, a 'coarse' table for the base composition point is generated. Depending on the values of MCP_j and p_{max}, each temperature value may, or may not, contain the MCP (see Fig. 1). The methodology of generating the table of tie-lines for a base point is given in Algorithm 1.

```
for each T value (Tj), where -1<j<NT
  for each p value (pi), where -1<i<Np
  {
      // provide initial guess for K-values
      if (p==p0 && T==T0)
          Get K-values from Wilson's correlation;
      else if (p==p0 && T!=T0)
          Use K-values from (0) and (j-1);
      else
          Use K-values from (i-1) and (j);
      Compute TL for z, pi and Tj;        // using standard EoS module
      if (trivial TL detected)            // using Eq. (4)
          Compute MCP for Tj;
          break;
  }
```

Algorithm 1: Pseudo-code for generating tie-line table

Since p and T of the compositions encountered in the course of a simulation (test points) are expected to be different from the discrete pressure and temperature levels of the $p-T$ grid, interpolation is required to obtain the closest approximation of the tie-line through a test point. The pressure and temperature indices ($\hat{i}$ and $\hat{j}$, respectively) for a given test point are obtained from:

$$0 < \frac{p - p_{min}}{\Delta p} - \hat{i} < 1, \tag{8}$$

$$0 < \frac{T - T_{min}}{\Delta T} - \hat{j} < 1, \tag{9}$$

where Δp and ΔT are defined by Eqs. (6) and (7), respectively. For $\forall (p,T) \in ([p_{\hat{i}}, p_{\hat{i}+1}], [T_{\hat{j}}, T_{\hat{j}+1}])$, bilinear interpolation in p and T is used:

$$\psi_{p, T_{\hat{j}, \hat{j}+1}} = \psi_{p_{\hat{i}}, T_{\hat{j}, \hat{j}+1}} + \delta p (\psi_{p_{\hat{i}+1}} - \psi_{p_{\hat{i}}})_{T_{\hat{j}, \hat{j}+1}}, \tag{10}$$

$$\bar{\psi}_{p,T} = \psi_{p, T_{\hat{j}}} + \delta T (\psi_{p, T_{\hat{j}+1}} - \psi_{p, T_{\hat{j}}}), \tag{11}$$

where ψ represents tie-line equilibrium compositions, and

$$\delta p = \frac{p - p_{\hat{i}}}{p_{\hat{i}+1} - p_{\hat{i}}}, \tag{12}$$

$$\delta T = \frac{T - T_{\hat{j}}}{T_{\hat{j}+1} - T_{\hat{j}}}. \tag{13}$$

Although standard EoS computations, which start from a rough approximation, involve the solution of highly nonlinear systems of equations; the overall structure of the two-phase binodal surface does not change significantly for $\forall (p,T) \in ([p_{\hat{i}}, p_{\hat{i}+1}], [T_{\hat{j}}, T_{\hat{j}+1}])$ with reasonably chosen Δp and ΔT. Therefore, the bilinear interpolation scheme described above is well behaved and provides accurate results.

The interpolated tie-line is not identical to the actual tie-line through the test point and is acceptable only if it is close to the test composition within a tolerance. The criteria given in Eq. (3) is used to verify the accuracy of the bilinear interpolation. If it is found that the test point is 'far' from the interpolated tie-line, a new table of tie-lines over the $p-T$ grid is generated. It is worth noting that this parameterization is different from the k-value tabulation approach, since it provides a thermodynamically consistent representation of the phase behavior. This consistency is provided when Eq. (3) is satisfied, for which the interpolated tie-lines are functions of p, T and compositions (Brantferger et al., 1991). Interpolation also provides continuous representation of the tie-lines as a function of these variables.

Several authors have studied phase behavior representation in the critical region. Michelsen (1984), for example, developed theoretical methods for calculation of critical points and near-critical phase boundaries for a multi-component mixture of specified composition. Parameterizing compositional space at pressure and temperature values just below the MCP loci is more challenging. This is because two nearby discrete temperature values have distinct MCPs. As a result, the bilinear interpolation technique introduced above is not directly applicable. Moreover, the thermodynamic behavior of two phases becomes identical when $p-T$ conditions are close to the critical loci. Since a majority of important thermal compositional problems have solution paths in the neighborhood of the critical surface, an effective and general interpretation of the near-critical region is required.

Since the length of the tie-lines tends to zero as the pressure gets closer to the *MCP* (Minimal Critical Pressure) of the mixture, interpolation using tie-line tables with large pressure intervals (coarse discretization) can lead to a poor approximation of the phase behavior. In order to resolve this issue, a refined table with small pressure intervals is constructed for the region just below the *MCP* (Voskov and Tchelepi, 2008b). Pressure intervals of the refined table decrease logarithmically as the pressure approaches the *MCP*:

$$(p_i)_j \quad = \quad \left(MCP_j + \left(\frac{\log i}{\log N_{refined}} - 1 \right) \Delta p_{refined} \right), \quad i \in \{1, N_{refined}\}, \tag{14}$$

where $\Delta p_{refined}$ defines the pressure support of the refined table and the number of near-critical tie-lines is given by $N_{refined}$. This tabulation improves the interpolation quality in the near-critical region quite significantly (Voskov and Tchelepi, 2008b). Obviously, the refined tabulation is not performed for T values that do not have an *MCP*. Fig. 1 summarizes possible table structures obtained using this methodology. In order to define the range of support for interpolation, an estimate of the
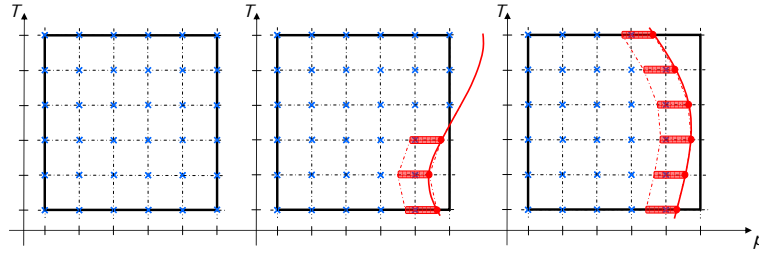

Figure 1: Tie-line table structure for a $p - T$ grid; none of the temperature values (left), some of them (center) or all of them (right) contain an MCP. Pressure and temperature bounds are defined by the black frame.

MCP for a given temperature is needed. We use linear interpolation in temperature for this purpose. For $\forall T \in [T_{\hat{j}}, T_{\hat{j}+1}]$, where both $T_{\hat{j}}$ and $T_{\hat{j}+1}$ have an *MCP*:

$$\overline{MCP} \quad = \quad MCP_{\hat{j}} + \delta T (MCP_{\hat{j}+1} - MCP_{\hat{j}}), \tag{15}$$

where δT is defined in Eq. (13) and $\hat{j}$ is given by Eq. (9). Pressure values above the interpolated *MCP* belong to the super-critical region.

A different interpolation technique is employed for the near-critical region. Noting that the tie-line length is zero at the *MCP*, and that the tie-line length increases gradually as one moves away from the *MCP*, we assume that the behavior of the tie-line length is similar to those at nearby temperature points. Therefore, we can interpolate in terms of the 'length' of the tie-lines. For this purpose, tie-lines with identical pressure indices from two refined tables (associated with nearby temperature values) are used for bilinear interpolation. The pressure index ($\hat{i}$) is chosen such that:

$$\log \hat{i} < (\frac{p - \overline{MCP}}{\Delta p_{refined}} + 1) \log N_{refined} < \log (\hat{i} + 1). \tag{16}$$

Using $\hat{i}$ in Eqs. (10) to (13), a modified bilinear interpolation in p and T is performed. This idea is shown in Fig. 2. The criterion of Eq. (3) is used to intersect the interpolated tie-line with the composition.
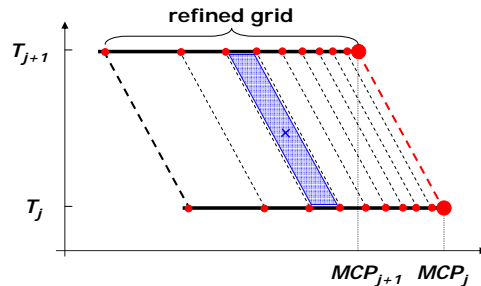

Figure 2: Refined interpolation, four tie-lines at the corners of the parallelogram are used for interpolation. Here, $N_{\mathbf{refined}} = 10$

Since in our parameterization framework, the effect of T is treated linearly in tie-line space, extension of isothermal SSC (Voskov and Tchelepi, 2008b) to thermal problems is straightforward. Interpolation in T is required before intersecting the critical tie-line with a test point:

$$\bar{\psi}_{cr} = \psi_{cr,T_{\hat{j}}} + \delta T(\psi_{cr,T_{\hat{j}+1}} - \psi_{cr,T_{\hat{j}}}), \tag{17}$$

where the critical compositions are represented by ψ_{cr}. The MCP associated with this interpolated critical tie-line is computed from Eq. (15). After performing the temperature interpolation defined by Eq. (17), the problem becomes 'isothermal' and therefore, an algorithm similar to that for the isothermal SSC can be used.

Parameterization for General-purpose Thermal Compositional Simulation

An effective tie-line based interpolation framework has been developed to parameterize general thermal-compositional problems. A composition is first checked in the table of critical tie-lines to identify its location relative to the critical surface. When the point needs to be checked in the sub-critical table, various strategies are employed to ensure that the best interpolation results are obtained. Below, we summarize this procedure.

Considering the fact that both coarse and refined tables are constructed for the near-critical region, one should first choose which table will be used for bilinear interpolation. For $p - T$ conditions, which have a refined table of tie-lines on one T side and a coarse table on the other side, a mixed interpolation in both tables is employed. Fig. 3 shows a schematic of two tie-line tables at temperatures T_j and T_{j+1}. Note that in the neighborhood of an MCP, a refined table is constructed. For a given composition at $T \in [T_j, T_{j+1}]$, we compute the MCP by interpolating between the two MCPs. For every composition at that temperature, we can use the appropriate coarse and/or refined tables for interpolation.
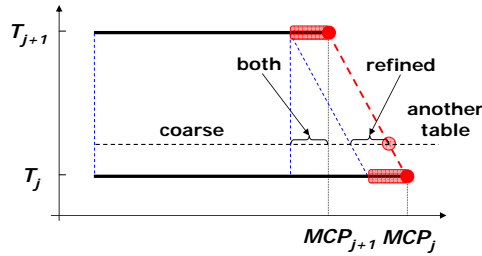

Figure 3: Sub-critical interpolation framework, test point could be anywhere along the horizontal dashed line

Note that if the separation in the temperature values is large, or the support of the refined table is small, it is possible that neither table would yield reasonable interpolation results. These issues are resolved by modifying the user-input interpolation parameters. The treatment in the near-critical region is performed only when two adjacent temperature values are associated with a critical tie-line and an MCP. Otherwise, interpolation using the coarse table is performed. The methodology for general-purpose thermal CSAT is presented in Algorithm 2.

```
for all tables of tie-lines
{
  if (hasMCP_{j-1} && hasMCP_j)
      Let MCP_min = min(MCP_{j-1}, MCP_j);
      Get MCP from Eq. (15);
      if (MCP < p)
          Next table;
      else if (MCP - Δp_refined < p < MCP)
          Interpolate in refined table;
      else if (MCP_min < p < MCP - Δp_refined)
          No support, Increase Δp_refined or  N_T;
      else if (MCP_min - Δp_refined < p < MCP_min)
          Interpolate in both tables;
  Interpolate in coarse table;
}
```

Algorithm 2: Pseudo-code for sub-critical tie-line table check

Isothermal CSAT, Application to a Field Problem

The implementation of CSAT for isothermal compositional problems has been tested on a field problem. In this section, we present performance studies of CSAT for the simulation of important recovery scenarios for large-scale problems.

Fig 4 shows a layout of the model used to test the isothermal CSAT algorithm. The fractured system is modeled using over a thousand discrete fractures (Gong et al., 2007). From more than 200,000 unstructured tetrahedral gridblocks of this model, almost 20% are in the fractures. The compositional fluid is represented using six components. First-contact miscible gas injection and depletion below the bubble-point pressure are considered in the presence of gravity effects.
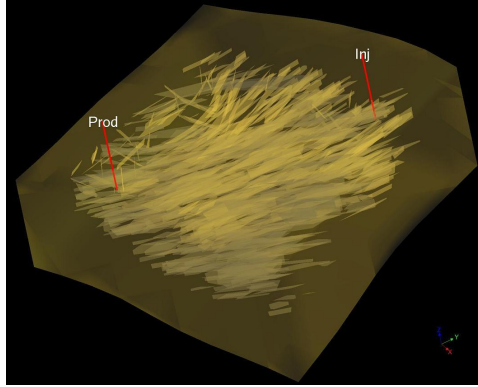

Figure 4: Fracture network of the model used for case studies

Table 1 represents performance results for the depletion simulation of this model at pressures below the bubble point. Apart from the EoS and solver times; CPU times for property calculation, linearization, initialization, etc. are also included in the total simulation time. Since the composition variation of the cells during simulation is relatively small for this depletion problem, parameterization of the compositional space around a limited number of composition points increases the efficiency of the simulation significantly. As indicated by Table 1, with almost the same number of Newton iterations, the EoS time for CSAT is orders of magnitude smaller than that of the standard approach. This effect is reflected in the total CPU time of the two simulations.

Table 1: CSAT efficiency for depletion below the bubble point, CPU time is reported in (hr:min)

Method	# TS	# Newton	Solver time	EoS time (% total)	Total time
standard	407	3070	15:22	42:16 (66.7)	63:24
CSAT	388	2929	12:09	00:17 (1.6)	17:14

We also study the applicability and efficiency of CSAT when the number of components used to represent the fluids increases. In order to obtain similar physical behaviors from the simulation of different number of components, we consider first-contact miscible injection on a coarser representation of the same model used in the previous example (with more than 5,000 cells). Table 2 summarizes the performance comparison of CSAT and standard methods. The computational gain in EoS time is more significant when the number of components is larger. A close examination of these results indicates that the speedup in terms of total CPU time is almost the same for the three scenarios. This is because increasing the number of components affects the solver portion of the fully implicit simulation significantly; as a result, EoS computations are no longer the most time-consuming component of the simulation. This argument is verified by observing that the non-EoS times of standard and CSAT approaches are almost the same for all cases and that the EoS time of CSAT is only a very small portion of the total CPU time.

Table 2: Isothermal CSAT vs. standard approach: sensitivity to the number of components, CPU time is reported in seconds

# of components	Method	# TS	# Newton	Solver time (% total)	EoS time (% total)	Total time
4	Standard	1282	6641	868 (33.8)	1,100 (42.8)	2,570
	CSAT	1282	6641	798 (58.2)	20 (1.5)	1,370
6	Standard	1323	5876	1,323 (33.3)	1,760 (44.3)	3,970
	CSAT	1323	5876	1,153 (58.5)	24 (1.2)	1,970
26	Standard	1481	6904	31,485 (44.0)	28,500 (39.9)	71,500
	CSAT	1481	6904	26,736 (74.2)	39 (0.1)	36,020

Thermal CSAT Accuracy, Case Study

An important strength of the tie-line based parameterization approach is that a compositional displacement problem normally takes place in a small portion of the compositional space (Voskov and Tchelepi, 2008a). Therefore, parameterization of the space along some base points at distinct pressure and temperature levels provides a reasonable representation of the phase behavior for the entire simulation. Thermodynamic phase behavior for the compositions of other cells in the problem (test points) is obtained using interpolation from nearby tie-lines. If necessary, interpolation in p and T is then used to precondition standard EoS calculations (Voskov and Tchelepi, 2008a,c). In order to show the accuracy of this strategy, one should first show how close these interpolated results are to standard EoS computations. Therefore, we first answer this question using a simple numerical experiment in the absence of hydrodynamic effects.

For this purpose, an 11-component mixture has been chosen (mixture III, Firoozabadi and Pan, 2002). Tie-lines in the coarse grid are computed (for $T = 640, 660\,°$R) from $p = 1,000\,psia$ with $\Delta p = 500\,psia$. Near-critical refinement is performed for a range of $1,000\,psia$ with 10 tie-lines. This table of tie-lines is used to provide initial guesses for standard negative flash of the same composition point at $T = 650°$R over the entire range of pressure (via interpolation in both p and T). The quality of the initial guess is then compared with that obtained from standard approaches; here, Wilson's correlation (Wilson, 1968) and phase stability tests (Michelsen, 1982a) are used as standard procedures. The number of flash iterations is normalized in terms of N_{Newton}, with $N_{SSI} \approx 0.7 N_{Newton}$, to compare the performance of different flash procedures (Firoozabadi and Pan, 2002).

Fig. 5 compares the number of normalized flash iterations for the different approaches. While the numerical results obtained from all four methods are practically identical, a large difference in the quality of the initial guess is observed. The number of flash iterations is about an order of magnitude larger when standard approaches are employed. The differences become more evident for near-critical pressures. We observe that although the flash procedure suffers from poor standard initial guesses for these pressures, interpolation results obtained from the refined table of tie-lines are very close to the actual EoS computations.
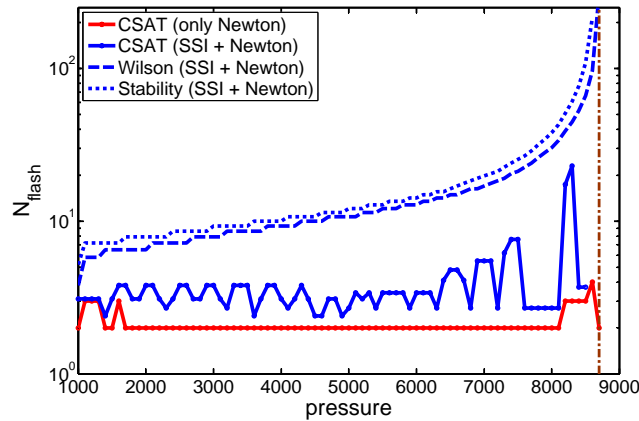

Figure 5: Negative flash with initial guess from space tabulation and standard procedures. Mixture's MCP is represented by the vertical dashed line.

Fig. 5 also reflects the structure of the coarse table of tie-lines. The number of flash iterations decreases at pressure values close to those computed via Eq. (5). In fact, interpolation results from the table of tie-lines can be used directly in Newton's method to perform the flash (a procedure which requires a good initial guess). It should be noted that since tie-line space tabulation provides excellent performance in determining the super-critical state, the comparisons are made all the way up to the mixture's *MCP*.

Similar behavior is observed when the temperature of the system is changed (Fig. 6). Although the number of flash iterations for the standard method increases in the near-critical region, little sensitivity is observed from interpolation at different temperatures in the near-critical region. Sensitivity to the difference in temperature values of the table is also studied for the same mixture (Fig. 7). The results obtained from interpolation are largely insensitive to the coarseness of the table of tie-lines in terms of temperature. This indicates that the general structure of the binodal surface changes almost linearly with temperature, even when the number of components is large. It should be noted that the interpolation-based flash fails to converge in the near-critical region, only if ΔT is very large.

Thermal CSAT, Application to Compositional Flow Simulation

In this section, we demonstrate the accuracy and efficiency of our approach. A general-purpose research simulator (Cao, 2002) is used to test the implementation outlined in the previous sections. An extensive set of examples for isothermal
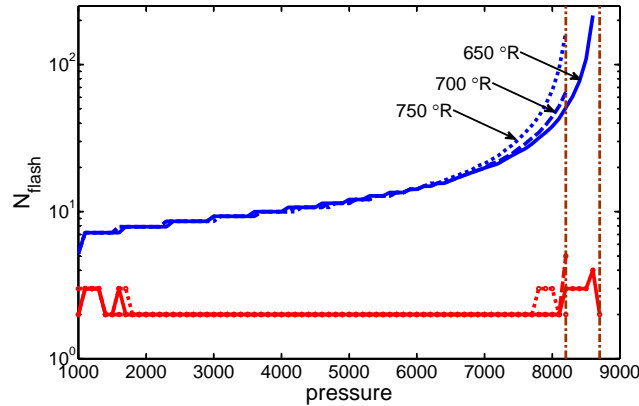
Figure 6: Negative flash with initial guess from space tabulation (red) and phase stability test (blue): sensitivity to temperature. Tables of tie-lines are computed at different temperatures. Mixture's MCP at different Ts are represented by the vertical dashed lines.
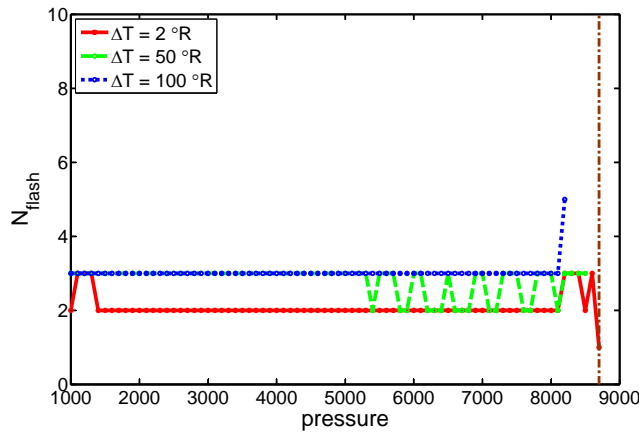

Figure 7: Space tabulation: sensitivity to coarseness in temperature tabulation. Newton's method is used to perform flash. Mixture's MCP is represented by the vertical dashed line.

implementation can be found in Voskov and Tchelepi (2007, 2008a,b).

Base Case I, First Contact Miscible Displacement. The first example is a first-contact miscible displacement problem. A mixture of $\{C_1(20\%), CO_2(80\%)\}$ at 810°R displaces $\{C_1(20\%), CO_2(5\%), C_4(30\%), C_{10}(45\%)\}$ at a reservoir temperature of 710°R. An injector and a producer operate under BHP control of 3800 and 3200 *psia*, respectively. A one-dimensional reservoir model with 100 cells is used, where the injector and producer are at opposite ends of the model. Fig. 8 shows the concentration profiles of the four components at $t = 0.5$ PVI, as well as the solution route in compositional space. The binodal surfaces at the initial and injection conditions (p and T) are plotted to highlight the nature of the solution path. It should be noted that both pressure and temperature change along the path. The solution indicates a continuous variation in compositions caused by physical transport and numerical dispersion along the route between the injector and producer, and that the path is mainly in the super-critical region.

Base Case II, Multi-contact Miscible Displacement. The second base case verifies the accuracy of the implementation for a multi-contact miscible displacement. Changing the initial and injection compositions of case I leads to a solution path such that it is partly in the super-critical space and partly in the subcritical region (Fig. 9). Similar to the isothermal CSAT examples in Voskov and Tchelepi (2008b), the solution path crosses the critical surface, but here, these surfaces are at different temperatures.

Standard Tests: Modified SPE3 and SPE5. We demonstrate the applicability of thermal CSAT using slight modifications of standard SPE tests: SPE3 (Kenyon and Behie, 1983) and SPE5 (Killough and Kossack, 1987). The first test is modified to represent a thermal gas-injection problem. For this purpose, a mixture of $\{C_1(70\%), C_2(30\%)\}$ at 650°R is injected into a 9-component initial oil at 530°R. The injector and producer are at opposite corners of the model operating
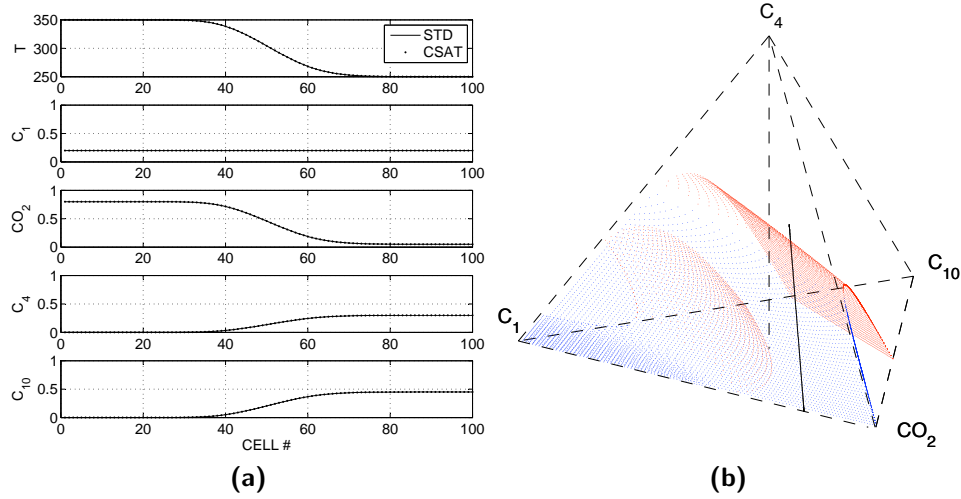
Figure 8: Base case I: (a) temperature and composition profiles, (b) solution path in compositional space with binodal surfaces at initial and injection conditions
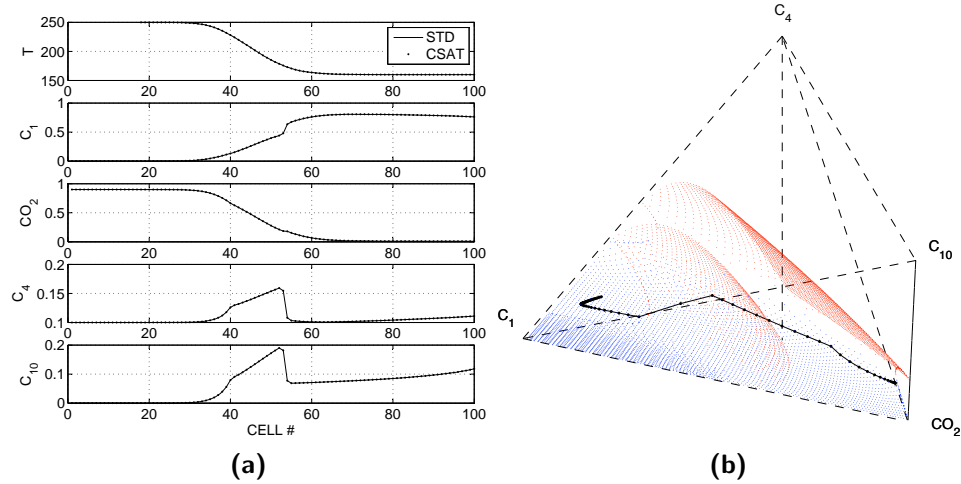

Figure 9: Base case II: (a) temperature and composition profiles, (b) solution path

under BHP constraints of 4000 and 2000 $psia$, respectively. For SPE5, five periods of water at 620°R ($\Delta t = 730$ days) and gas $\{C_1(77\%), C_3(20\%), C_6(3\%)\}$ at 600°R ($\Delta t = 100$ days) are injected into a 6-component oil at 520°R. The injector and producer operate at 5000 and 3000 $psia$, respectively.

We study the impact of grid size on the efficiency of thermal CSAT compared to a conventional approach. Simulations are performed by refining the horizontal layers of the model. A rough idea about the distribution of the simulation composition points over the $p - T$ grid can be obtained from Table 3. For SPE3, almost 80% of the compositions are identified via interpolation using the critical surface. The remaining compositions lie along extensions of sub-critical tie-lines. However, for SPE5, the compositions are essentially in the subcritical space.

These examples demonstrate the robustness of thermal CSAT for the entire compositional space, since the encountered compositions exist in both super- and sub-critical regions as well as the near-critical region. As a result, application of CSAT reduces the cost of phase stability tests during simulation (Table 3), and leads to orders of magnitude speedup in the EoS portion of the computations (Fig. 10).

Parameterization of the Multi-phase Thermal Compositional Problem

Compositional space parameterization techniques can be extended to three-phase problems. For such displacements, tie-triangles as well as tie-lines, are the underlying parameterization tools (Voskov and Tchelepi, 2008c). A robust bisection-

Table 3: Distribution of compositions ($\times 10^5$, % total in parentheses) determined by interpolation in critical and sub-critical tie-lines for SPE3 (top) and SPE5 (bottom). The ratio (standard/CSAT) of SSI and Newton stability iterations is given in the last two columns.

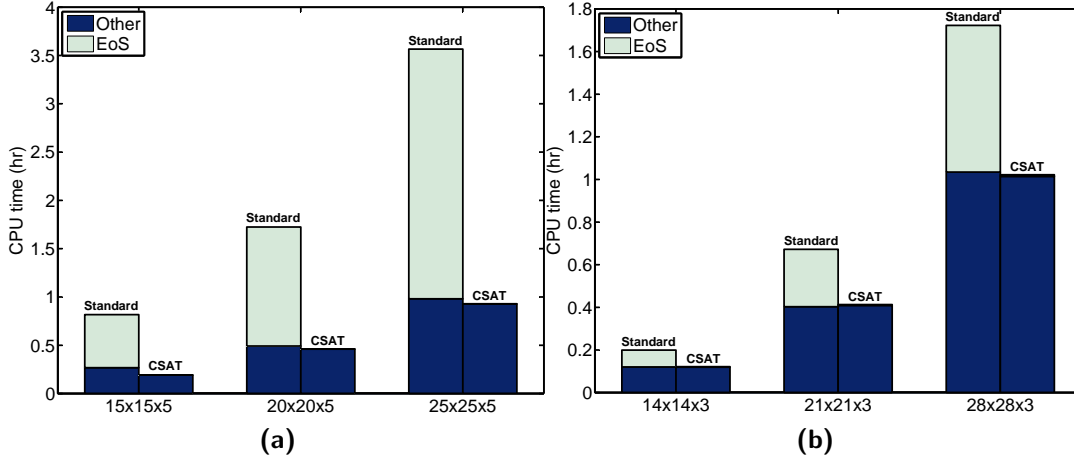| Grid size	Critical	Sub-critical	EoS-SSI	EoS-Newton
$15 \times 15 \times 5$	19.2 (79.2)	5.0 (20.8)	858	189
$20 \times 20 \times 5$	41.5 (79.2)	10.9 (20.8)	1152	263
$25 \times 25 \times 5$	85.0 (80.7)	20.3 (19.3)	1574	367
$14 \times 14 \times 3$	5.0 (21.2)	18.5 (78.8)	513	374
$21 \times 21 \times 3$	15.8 (19.6)	64.6 (80.4)	1144	829
$28 \times 28 \times 3$	39.0 (18.8)	168.4 (81.2)	1950	859

Figure 10: Thermal CSAT performance for SPE3 (a) and SPE5 (b), EoS time for CSAT based simulations is a weak function of grid size

based methodology for the solution of a three-phase negative flash procedure has been developed. It can be shown that for a system with constant K-values, a given composition point in compositional space is parameterized by a unique tie-triangle, regardless of its location in the single-, two-, or three-phase region. The three-phase negative flash enables us to compute such a tie-triangle.

We first present the accuracy of tie-triangle tabulation and interpolation for three-phase systems. For this purpose, we perform computations for a mixture with a constant composition. We use a 10-component mixture composed of 80% of the SPE3 fluid (Kenyon and Behie, 1983) and 20% water. The mixture is flashed at $T = 370\,\mathrm{K}$ and from $p = 10\,bar$ all the way up to the MCP. By definition, a tie-triangle becomes critical, when any of its sides (here, oil and vapor sides) coincide. Tie-triangles in the coarse grid are computed (for $T = 370\,\mathrm{K} \pm \Delta T/2$) from $p = 10\,bar$ with $\Delta p = 10\,bar$. Near-critical refinement is performed for a range of $30\,bar$ with 25 tie-lines. Fig. 11 compares the quality of the initial guess obtained from interpolation and correlation (Peng and Robinson, 1976):

$$K_{w,i} = \frac{y_i}{w_i} = 10^6 \frac{p_{c,i}T}{T_{c,i}p}, \qquad i \in \{1, N_c\}, \tag{18}$$

and $K_i = y_i/x_i$ is given by Wilson's correlation (Wilson, 1968). Interpolation results are directly passed to the Newton flash iteration, whereas both SSI and Newton iterations are employed for the initial guess from correlation. The number of flash iterations is normalized in terms of Newton flash iterations. The plot of the oil-phase ratio indicates that the composition lies outside the tie-triangle for near-critical pressures. Similar to Fig. 5, interpolation-based negative-flash computations converge faster for the entire pressure range. This is specially the case for near-critical pressures, where the correlation-based flash fails to converge, while refined tabulation in tie-triangle space provides a very close approximation.

We next consider parameterization of the subcritical space along a composition route. A given composition is first checked in the table of existing tie-triangles. The thermodynamic state of the composition is confirmed if the three-phase table check returns a three-phase state. Otherwise, the point is checked in the table of existing tie-lines to confirm if it is in a single-, or two-phase state. This is because the three-phase table check is not sufficient to determine wether the point is in the single-, or two-phase region. A new table of tie-triangles with/without tie-lines is constructed for the composition, if it is not parameterized by existing tie-triangles and tie-lines. Fig. 12 illustrates two examples of composition route parameterization for a three-phase immiscible displacement. The path between the end-points is divided into 100 points, each of which is
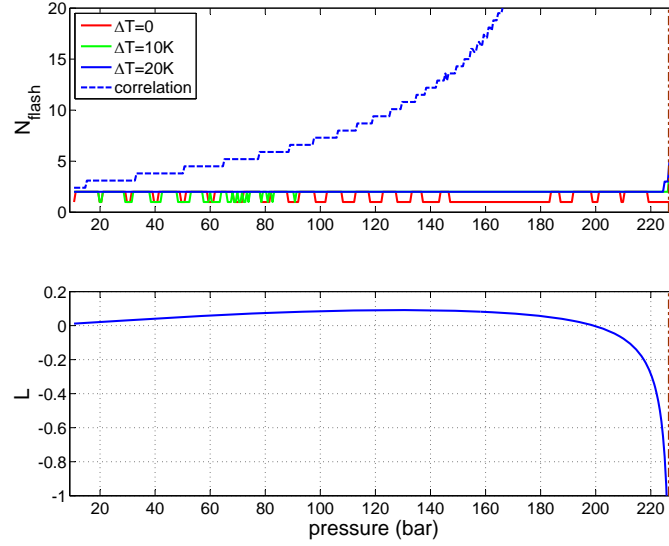
Figure 11: Top: Negative three-phase flash with initial guess from space tabulation and correlation. Correlation-based flash fails to converge at $p = 210\,bar$; Bottom: oil phase ratio of the constant composition. Mixture's MCP is represented by the vertical dashed line.

parameterized by a tie-triangle, or a tie-line. The tables of tie-triangles and tie-lines are constructed at two discrete p and T values. The pressure and temperature are constant along the path and are equal to the average discrete values. We perform adaptive tabulation for each composition along the path. Interpolation in existing tables is performed for both p and T.
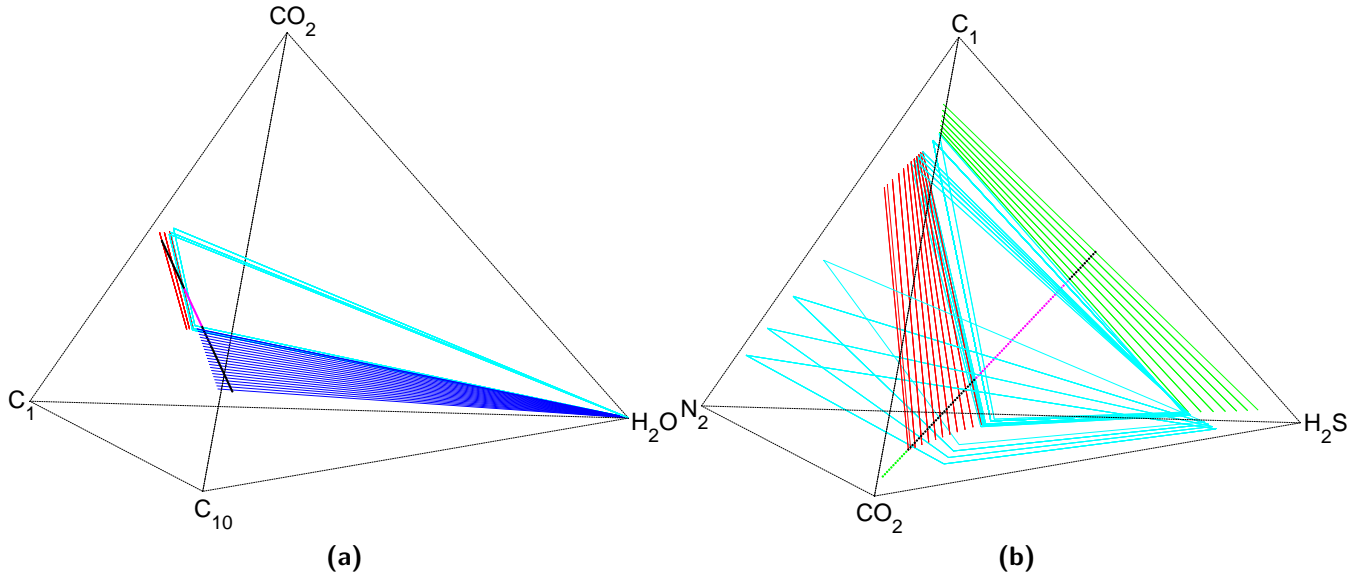

(a)   **(b)**

Figure 12: Compositional space parameterization for immiscible three-phase systems: **(a)** $\{H_2O, C_{10}, CO_2, C_1\}$ **with end-points** $\{0.05, 0.7, 0.2, 0.05\}$, $\{0.01, 0.06, 0.45, 0.48\}$ **and** $p = 150\,bar$, $T = 400\,K$. **(b)** $\{H_2S, CO_2, C_1, N_2\}$ **with end-points** $\{0.03, 0.9, 0.03, 0.04\}$, $\{0.45, 0.05, 0.45, 0.05\}$ **and** $p = 100\,bar$, $T = 140\,K$. **Green, black and magenta dots represent compositions in the oil-, two- and three-phase regions, respectively. Oil-liquid, oil-gas, and liquid-gas tie-lines are in blue, red, and green, respectively.**

The three- and single-phase compositions in the plots of Fig. 12 are parameterized by tie-triangles only. The compositions in the two-phase region are parameterized by tie-lines in the oil-gas, oil-liquid, or liquid-gas regions. It is worth noting that the number of tie-lines, or tie-triangles, is much smaller than the number of compositions that they parameterize, and that the path in Fig. 12-b traverses single-, two-, and three-phase regions.

We finally present preliminary results for the application of CSAT to three-phase compositional simulation. For this purpose, we add water to the system and use a simplified thermodynamic behavior, where the water and oil phases contain only water and hydrocarbons, respectively. The fraction of the water component in the vapor phase is obtained from a

correlation (Tortike and Farouq Ali, 1989). The details of the modified negative flash for EoS computations are presented in the Appendix.

We simulate injection of $60\% CO_2, 10\% C_1$ and $30\% H_2O$ into a mixture composed of $1\% CO_2, 19\% C_1, 60\% C_{16}$ and $20\% H_2O$. The injector and producer operate at 150 and 90 bars, respectively, and are placed at opposite corners of the reservoir ($100m \times 100m \times 1m$, with $144 \times 1 \times 1$ and $12 \times 12 \times 1$). The amount of steam in the vapor phase at initial conditions is approximately 15%. Fig. 13 shows the solution path between the injection and initial compositions, as well as the tie-triangles that parameterize the space at the initial reservoir pressure (120 bar).
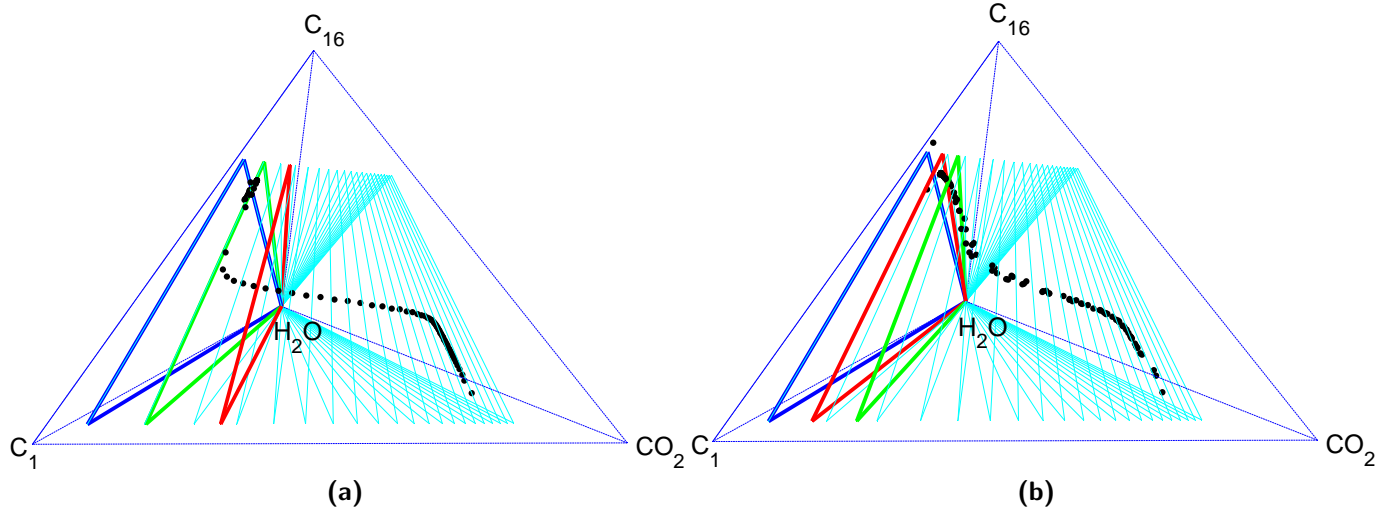

Figure 13: Solution path, represented by black dots, for 1D (a) and 2D (b) simulation after identical cumulative gas injected. Tie-triangles parameterizing the space at p_{initial} are in cyan, while tie-triangles computed by CSAT are in different colors.

The compositions are obviously smeared along the solution path in the two-dimensional simulation. Four and five tables of tie-triangles are computed for two- and one-dimensional cases, respectively. The tables that are most frequently used for interpolation are located around compositions which require a stability test. The cumulative usage of the tie-triangles in the course of simulation (Fig. 14) indicates that for the 1D case, space tabulation takes place in the early stages of the gas injection process, and after the development of the one-dimensional front, one table is used, almost exclusively, for the rest of the simulation. While in the 2D case, different tables are computed and used for interpolation with the evolution of the two-dimensional displacement front.
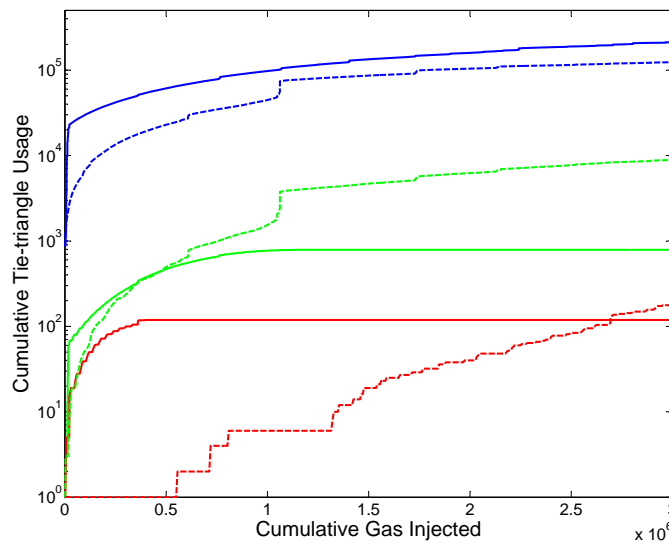

Figure 14: Cumulative usage of tie-triangle tables for 1D (solid) and 2D (dashed) simulations. The color of the curves corresponds to the tie-triangles in Fig. 13.

Conclusions

The applicability and effectiveness of the compositional space adaptive tabulation (CSAT) method for isothermal compositional reservoir simulation have been validated for a field-scale compositional problem. We described the extension of this tie-line based parameterization framework to thermal-compositional problems. The accuracy and efficiency of our general-purpose approach have been demonstrated using a number of challenging test problems. The CSAT framework yields very accurate treatment of the entire compositional space and is orders of magnitude faster than standard approaches in terms of EoS (Equation of State) time, which is the dominant time consuming kernel of standard compositional simulation. With CSAT, our results indicate that even for challenging compositional problems with large numbers of components, the EoS computational cost is a very small fraction of the total time.

Different techniques are used to parameterize immiscible and multi-contact miscible displacements. The proposed approach for parameterization of the sub-critical space is motivated by theoretical findings from method-of-characteristics solutions of ideal problems, where tie-lines play a key role in the solution construction. In our approach, tie-lines are used to parameterize the phase behavior, and pressure/temperature interpolation in this tie-line space is employed. The approach is effective in the presence of a wide range of complexities in immiscible gas injection simulations.

A critical surface is adaptively constructed and used to identify if a composition is sub- or super-critical at the prevailing pressure and temperature conditions. If a composition is sub-critical, tie-line parameterization is used. If the composition is super-critical, interpolation of the critical tie-lines is used to identify if the phase is liquid-like or gas-like. The idea of parameterizing the critical surface has been extended to thermal problems, and we show that pressure and temperature effects can be handled in a robust and efficient manner in our CSAT framework.

We have also extended the framework of compositional space parameterization to the three-phase problem. Using a robust negative flash procedure, the sub-critical three-phase compositional space is parameterized in terms of tie-triangles and/or tie-lines. We have shown that interpolation in tie-triangle/tie-line tables provides accurate representation of the phase behavior. Apart from the efficiency gains, the insight obtained from this approach allows for a fundamental understanding of the workings of various thermal compositional displacement processes in large-scale simulations.

Nomenclature

H_j	enthalpy of phase j
$\hat{i}$	index of a given composition in regular/refined p table
$\hat{j}$	index of a given composition in T table
K_i	phase equilibrium ratio of component i (y_i/x_i)
$K_{w,i}$	phase equilibrium ratio of component i (y_i/w_i)
N_c	total number of components
N_p	number of discretization points in the coarse p table
N_T	number of discretization points in the T table
p	pressure
$p_{c,i}$	critical pressure of component i
q_j	source/sink term for phase j
S_j	saturation of phase j
t	time
T	temperature
$\mathbf{u}_j$	Darcy velocity vector of phase j
U_j	internal energy of phase j
U_R	rock internal energy
w_i	mole fraction of component i in water phase
x_i	mole fraction of component i in oil phase
$x_{i,j}$	mole fraction of component i in phase j
y_i	mole fraction of component i in vapor phase
ε	tolerance for checking the closeness of a composition to an interpolated tie-line
κ	thermal conductivity
ρ_j	density of phase j
ϕ	porosity

Acknowledgements

References

Brantferger, K.M., Pope, G.A. and Sepehrnoori K.: "Development of a Thermodynamically Consistent, Fully Implicit, Equation-of-State, Compositional Steamflood Simulator", SPE 21253, The 11th SPE Symposium on Reservoir Simulation, Anaheim, CA (1991).

Cao, H.: *Development of Techniques for General Purpose Simulators*, PhD thesis, Stanford University, (2002).

Chien, M.C.H., Yardumian, H.E., Chung E.Y. and Todd, W.W.: "The Formulation of a Thermal Simulation Model in a Vectorized, General Purpose Reservoir Simulator", SPE 18418, The Tenth SPE Symposium on Reservoir Simulation, Houston, TX (1989).

Coats,K.H.,George, W.D., Chu, C. and Marcum, B.E.: "Three-Dimensional Simulation of Steamflooding", *Soc. Pet. Eng. J.* (Dec. 1974) 573-592.

Coats, K.H.: "Simulation of Steamflooding With Distillation and Solution Gas", *Soc. Pet. Eng. J.* (Oct. 1976) 235-247.

Dindoruk, B., Johns, R.T. and Orr, F.M., Jr.: "Analytical Solution for Four Component Gas Displacement with Volume Change on Mixing", June (1992) Third European Conference on the Mathematics of Oil Recovery, Delft, Holland.

Entov, V.M.: "Nonlinear Waves in Physicochemical Hydrodynamics of Enhanced Oil Recovery. Multicomponent Flows", Proceedings of the International Conference "Porous Media: Physics, Models, Simulations", Moscow, Russia, 19-21 Nov., (1997).

Entov, V.M., Turetskaya, F.D., and Voskov, D.V.: "On Approximaion of Phase Equilibria of Multicomponent Hydrocarbon Mixtuers and Prediction of Oil Displacements by Gas Injection", Eighth European Conference on the Mathematics of Oil Recovery, Freiburg, Germany, 4-7 Sep., (2001).

Farouq Ali, S.M. and Abou-Kassem, J.: "Simulation of Thermal Recovery Processes", In: Proceedings of the 1st and 2nd International Forum on Reservoir Simulation, Alpbach, Austria, September 12-16, 1988 and September 4-8, 1989.

Firoozabadi, A., and Pan, H.: "Fast and Robust Algorithm for Compositional Modeling: Part I: Stability Analysis Testing", SPE Journal Mar. (2002), **7**, 78-89.

Gong, B., Karimi-Fard, M., and Durlofsky, L.J.: "An Upscaling Procedure for Constructing Generalized Dual-porosity/Dual-permeability Models from Discrete Fracture Characterizations", SPE 102491, 2007 SPE Annual Technical Conference and Exhibition, San Antonio, TX, Sep. 24-27.

Helfferich, F.G.: "Theory of Multicomponent, Multiphase Displacement in Porous Media", *Soc. Pet. Eng. J.* (February 1981) **271**, 51-62.

Jessen, K.R., Wang, Y., Ermakov, P., Zhu, J., and Orr, F.M., Jr.: "Fast, Approximate Solutions for 1D Multicomponent Gas Injection Problems", SPE 56608, SPE Annual Technical Conference and Exhibition, Houston, TX, (Oct. 1999).

Kenyon, D., and Behie, G.A.: "Third SPE Comparative Solution Project: Gas Cycling of Retrograde Condensate Reservoirs", SPE 11278, proceedings of the seventh SPE Symposium on Reservoir Simulation, San Francisco, CA, Nov. 15-18, (1983).

Killough, J.E., and Kossack, C.A.: "Fifth Comparative Solution Project: Evaluation of Miscible Flood Simulators", SPE 16000, The Ninth SPE Symposium on Reservoir Simulation, San Antonio, TX (1987).

Michelsen, M.L.: "The Isothermal Flash Problem: Part I. Stability", *Fluid Phase Equilibria* (1982a) **9**, 1-19.

Michelsen, M.L.: "The Isothermal Flash Problem: Part II. Phase-split Calculation", *Fluid Phase Equilibria* (1982b) **9**, 21-40.

Michelsen, M.L.: "Calculation of Critical Points and Phase Boundaries in the Critical Region", *Fluid Phase Equilibria* (1984) **16**, 57-76.

Monroe, W.W., Silva, M.K., Larsen, L.L. and Orr, F.M., Jr: "Composition Paths in Four-Component Systems: Effect of Dissolved Methane on 1D CO_2 Flood Performance", *SPE Reservoir Engineering* (1990) **5**, 423-432.

Orr, F.M., Jr.: *Theory of Gas Injection Processes*, Tie-Line Publications, Copenhagen, Denmark (2007).

Peng, D.Y. and Robinson, D.B.: "Two and Three-Phase Equilibrium Calculations for Systems Containing Water", *Can. J. Chem. Eng.*, (1976), **54**, 595-598.

Tortike, W.S. and Farouq Ali, S.M.: "Saturated-Steam-Property Functional Correlations for Fully Implicit Thermal Reservoir Simulation," *SPERE* (November 1989) 471; *Trans.*, AIME, **287**.

Voskov, D.V., and Entov, V.M.: "Problem of Oil Displacement by Gas Mixtures", *Fluid Dynamics*, (2001) **36**, No. 2, 269-278.

Voskov, D.V.: *Two-phase Multicomponent Flows Through Porous Media*, PhD thesis, Gubkin Russian State Oil and Gas University, Moscow, Russia, (2002).

Voskov, D.V., and Tchelepi, H.: "Compositional Space Parameterization for Miscible Displacement Simulation", *Transport in Porous Media*, (2007), DOI: 10.1007/s11242-008-9212-1

Voskov, D.V., and Tchelepi, H.: "Compositional Space Parameterization: Theoretical Background and Application for Immiscible Displacements", *SPE Journal* (2008a), (paper SPE 106029 presented at 2007 SPE Reservoir Simulation Symposium, Woodlands, TX, February 26-28).

Voskov, D.V., and Tchelepi, H.: "Compositional Space Parameterization: Multi-Contact Miscible Displacements and Extension to Multiple Phases", *SPE Journal* (2008b), (paper SPE 113492 presented at 2008 SPE/DOE Symposium on Improved Oil Recovery, Tulsa, Oklahoma, April 20-23).

Voskov, D.V., and Tchelepi, H.: "Tie-simplex Based Framework for General Multi-phase Thermodynamic Equilibrium Computations", 11th European Conference on the Mathematics of Oil Recovery, Bergen, Norway, 8-11 Sep., (2008c).

Wang, Y. and Orr, F.M., Jr.: "Analytical Calculation of Minimum Miscibility Pressure", *Fluid Phase Equilibria* (1997) **139**, 101-124.

Wilson, G.: "A Modified Redlich-Kwong EOS, Application to General Physical Data Calculations", Paper 15C presented at the Annual AIChE National Meeting held in Cleveland, Ohio, May 4-7, 1968.

Wong, T.W. and Aziz K.: "Considerations in the Development of Multipurpose Reservoir Simulation Models", In: Proceedings of the 1st and 2nd International Forum on Reservoir Simulation, Alpbach, Austria, September 12-16, 1988 and September 4-8, 1989.

Zhu, J.: *Multicomponent Multiphase Flow in Porous Mdedia with Temperature Variation or Adsorption*, PhD thesis, Stanford University, (2003).

Solution of Modified Three-phase Negative Flash

Mass balance for every component that partitions in the oil, vapor, and water phases (with phase ratios denoted by L, V and W respectively) is given by:

$$z_i = x_i L + y_i V + w_i W, \qquad i \in \{1, N_c\}.$$

This equation is valid when a phase is not present, for which the phase ratio becomes negative. For hydrocarbon components (with subscript h), we assume $w_h = 0$, therefore:

$$z_h = x_h L + y_h V, \qquad h \in \{1, N_h\},$$

which yields:

$$x_h = \frac{z_h}{L(1 - K_h) + K_h(1 - W)}, \qquad h \in \{1, N_h\}, \tag{A-1}$$

where $K_{h \in \{1, N_h\}} = y_h / x_h$. For the water component,

$$z_w = y_w V + W,$$

from which, one obtains:

$$W = \frac{z_w + y_w(L - 1)}{1 - y_w}. \tag{A-2}$$

Using W from Eq. (A-2) in Eq. (A-1), yields:

$$x_h = \frac{z_h(1 - y_w)}{(1 - y_w - K_h)L + K_h(1 - z_w)}, \qquad h \in \{1, N_h\}. \tag{A-3}$$

The target function is:

$$f(L) = \sum_{i=1}^{N_c}(y_i - x_i) = \sum_{h=1}^{N_h}(y_h - x_h) + y_w = 0,$$

which from Eq. (A-3), takes the form:

$$f(L) = \sum_{h=1}^{N_h} \frac{z_h(1 - y_w)(K_h - 1)}{(1 - y_w - K_h)L + K_h(1 - z_w)} + y_w = 0. \tag{A-4}$$

The problem is to solve $f(L) = 0$ in the physical region for L given by $L_{min} < L < L_{max}$. $f(L)$ has N_h asymptotes given by:

$$\hat{L}_h = \frac{K_h(z_w - 1)}{1 - y_w - K_h}, \qquad h \in \{1, N_h\}. \tag{A-5}$$

Differentiating $f(L)$ yields:

$$\frac{\partial f(L)}{\partial L} = \sum_{h=1}^{N_h} \frac{z_h(1 - y_w)(1 - K_h)(1 - y_w - K_h)}{[(1 - y_w - K_h)L + K_h(1 - z_w)]^2}. \tag{A-6}$$

If y_w is sufficiently small, $\frac{\partial f(L)}{\partial L}$ will be positive and consequently, $f(L)$ will be monotonically increasing between adjacent asymptotes. Therefore, a bisection-based algorithm can be used to solve for $f(L) = 0$.

Since $x_h > 0$ must be satisfied in Eq. (A-3), physical bounds on L can be obtained from:

$$L_{min} = \max(\hat{L}_h) \qquad \text{if} \qquad 1 - y_w - K_h > 0, \tag{A-7}$$

$$L_{max} = \min(\hat{L}_h) \qquad \text{if} \qquad 1 - y_w - K_h < 0, \tag{A-8}$$

where $\hat{L}_h$ is defined in Eq. (A-5). Obviously, $f(L)$ will not have a solution if $L_{max} < L_{min}$. Otherwise, a bisection-based algorithm can be used to locate the solution to Eq. (A-4). Fig. 15 compares the accuracy of this modified negative flash (against three-phase negative flash) for a 10-component mixture composed of 80% of the SPE3 mixture and 20% water at various pressures and temperatures.
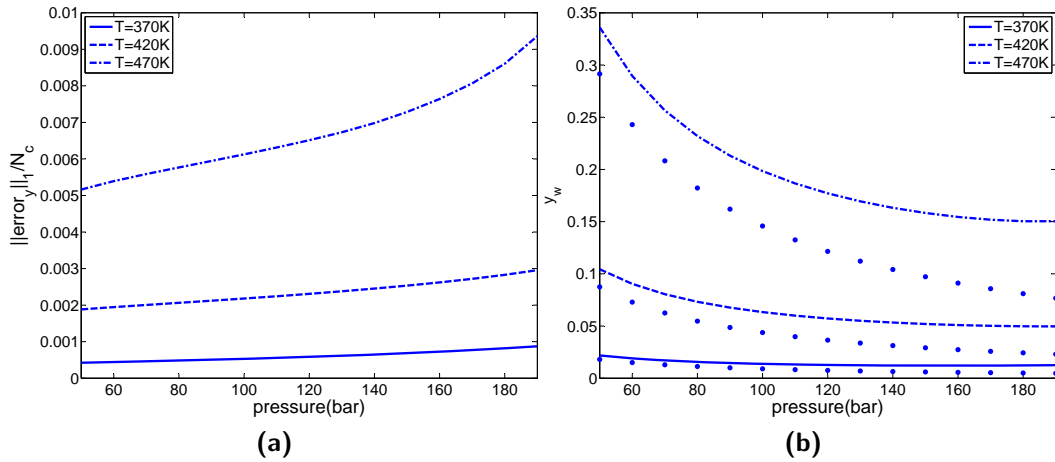

Figure 15: (a) accuracy of the steam flash, (b) steam fraction from three-phase flash (lines) and correlation (Tortike and Farouq Ali, 1989) (dots).